The Journal of Immunology

RESEARCH ARTICLE | FEBRUARY 15 2013

GM-CSF Produced by Nonhematopoietic Cells Is Required for Early Epithelial Cell Proliferation and Repair of Injured Colonic Mucosa

Laia Egea; ... et. al

J Immunol (2013) 190 (4): 1702–1713.
https://doi.org/10.4049/jimmunol.1202368

GM-CSF Produced by Nonhematopoietic Cells Is Required for Early Epithelial Cell Proliferation and Repair of Injured Colonic Mucosa

Laia Egea,* Christopher S. McAllister,* Omar Lakhdari,* Ivelina Minev,* Steve Shenouda,* and Martin F. Kagnoff*,†

GM-CSF is a growth factor that promotes the survival and activation of macrophages and granulocytes, as well as dendritic cell differentiation and survival in vitro. The mechanism by which exogenous GM-CSF ameliorates the severity of Crohn's disease in humans and colitis in murine models has mainly been considered to reflect its activity on myeloid cells. We used GM-CSF–deficient (GM-CSF$^{-/-}$) mice to probe the functional role of endogenous host-produced GM-CSF in a colitis model induced after injury to the colon epithelium. Dextran sodium sulfate (DSS), at doses that resulted in little epithelial damage and mucosal ulceration in wild type mice, caused marked colon ulceration and delayed ulcer healing in GM-CSF$^{-/-}$ mice. Colon crypt epithelial cell proliferation in vivo was significantly decreased in GM-CSF$^{-/-}$ mice at early times after DSS injury. This was paralleled by decreased expression of crypt epithelial cell genes involved in cell cycle, proliferation, and wound healing. Decreased crypt cell proliferation and delayed ulcer healing in GM-CSF$^{-/-}$ mice were rescued by exogenous GM-CSF, indicating the lack of a developmental abnormality in the epithelial cell proliferative response in those mice. Nonhematopoietic cells, and not myeloid cells, produced the GM-CSF important for colon epithelial proliferation after DSS-induced injury, as revealed by bone marrow chimera and dendritic cell–depletion experiments, with colon epithelial cells being the cellular source of GM-CSF. Endogenous epithelial cell–produced GM-CSF has a novel nonredundant role in facilitating epithelial cell proliferation and ulcer healing in response to injury of the colon crypt epithelium. ***The Journal of Immunology*****, 2013, 190: 1702–1713.**

Granulocyte-macrophage CSF is a cytokine that promotes survival and activation of macrophages, neutrophils, and eosinophils, and it stimulates dendritic cell (DC) maturation in vitro (1). GM-CSF signals through a heterodimeric receptor that has an α subunit (GM-CSFRα, CD131) specific for GM-CSF binding and a signaling βc subunit (GM-CSFRβc, CD116) that is shared with the receptors for IL-3 and IL-5 in humans (2).

The role of GM-CSF in intestinal mucosal homeostasis is not fully understood (3). GM-CSF is expressed by epithelial cells in the small intestine of the mouse (4, 5), by rat Paneth cells (6), by colon cancer cell lines (7, 8), and by human colon cancer biopsies (8). It is also found in mucosal lesions of inflammatory bowel disease patients (9, 10). However, GM-CSF is expressed at low levels, if at all, in normal mouse or human colon in vivo (8, 11). Recent studies indicated that GM-CSF can influence the differentiation and survival of mouse intestinal DCs (11–13); however, mice lacking GM-CSF do not manifest altered DC numbers or a constitutive phenotype in the intestine (11, 14). In contrast, we found that mice deficient in GM-CSF had a greater bacterial burden, increased mucosal inflammation, systemic spread of infection, and delayed pathogen clearance postinfection with the epithelial cell attaching/effacing enteric pathogen *Citrobacter rodentium* (11). In that model, GM-CSF–mediated host protection postinfection was associated with increased survival of mucosal DCs and localization of DCs to the subepithelial region of the infected colon (11). In addition, mice deficient in GM-CSF were more susceptible to ileal injury and inflammation induced by nonsteroidal anti-inflammatory drugs (NSAIDs) (15) and colitis induced by high doses of dextran sodium sulfate (DSS) (14), an agent that causes epithelial injury and subsequent inflammation in the colon (16–18). However, the role and the cellular sources of GM-CSF in the injured colon and the mechanism by which GM-CSF$^{-/-}$ mice develop more severe disease in a DSS-induced colitis model remain unknown.

Administration of GM-CSF has been studied extensively as a therapy for its effects on hematopoietic cells. However, it is also known that receptors for GM-CSF are expressed at levels similar to those of monocytes on isolated human intestinal epithelial cells (IECs) (19). Exogenous GM-CSF treatment in DSS-induced colitis in mice ameliorated the severity of the colitis and promoted colonic mucosal healing by mechanisms thought to involve myeloid cells (20, 21). Cells of the hematopoietic lineage were also important in GM-CSF–facilitated epithelial repair after LPS-induced acute lung injury (22) and NSAID-induced ileitis in mice (15).

*Laboratory of Mucosal Immunology, Department of Medicine, University of California, San Diego, La Jolla, CA 92093; and †Department of Pediatrics, University of California, San Diego, La Jolla, CA 92093

Received for publication August 24, 2012. Accepted for publication December 5, 2012.

This work was supported by National Institutes of Health Grant DK35108 and a grant from the William K. Warren Foundation. The Biomedical Genomics laboratory is supported by National Institutes of Health Grants DK063491, CA023100, and DK080506; and the University of California, San Diego Neuroscience Microscopy Shared Facility is supported by Grant P30 NS047101.

The datasets presented in this article have been submitted to the National Center for Biotechnology Information/Gene Expression Omnibus (http://www.ncbi.nlm.nih.gov/geo/query/acc.cgi?acc=GSE42173) under accession number GSE42173.

Address correspondence and reprint requests to Prof. Martin F. Kagnoff, University of California, San Diego, 9500 Gilman Drive, Mail Code 0623D, La Jolla, CA 92093-0623. E-mail address: mkagnoff@ucsd.edu

The online version of this article contains supplemental material.

Abbreviations used in this article: BM, bone marrow; DC, dendritic cell; DSS, dextran sodium sulfate; DTR, diphtheria toxin receptor; DTX, diphtheria toxin; FDR, false discovery rate; GO, gene ontology; hpf, high-power field; IEC, intestinal epithelial cell; mGM-CSF, mouse GM-CSF; MPO, myeloperoxidase; NSAID, nonsteroidal anti-inflammatory drug; WT, wild type.

We postulated that endogenous host GM-CSF may have an important protective role during mucosal injury in the colon in vivo by facilitating repair of the injured epithelial lining. As a model of injury, we used colitis induced by DSS in mice deficient in GM-CSF and wild type (WT) mice. GM-CSF$^{-/-}$ mice developed greater epithelial damage and delayed ulcer healing compared with WT mice. To gain insight into the mechanism by which GM-CSF facilitates epithelial repair, we performed whole-genome expression analysis using GM-CSF$^{-/-}$ or WT isolated colonic crypts. To determine the cellular source of GM-CSF responsible for epithelial repair, we depleted DCs and generated bone marrow (BM) chimeras. We report that GM-CSF produced by nonhematopoietic cells, and specifically epithelial cells in the colon, has a novel and nonredundant role in promoting colon crypt epithelial cell proliferation and ulcer healing in response to epithelial injury.

Materials and Methods

Mice

C57BL/6 (WT) and TNFα$^{-/-}$ mice were from The Jackson Laboratory. GM-CSF and GM-CSF receptor βc deficient (GM-CSF$^{-/-}$ and GM-CSFRβc$^{-/-}$) mice were provided by Dr. B. Trapnell (Children's Hospital Medical Center, Cincinnati, OH). Mice were maintained at the University of California, San Diego animal facility, which is accredited by the American Association for Accreditation of Laboratory Animal Care. All animal protocols were approved by the University of California, San Diego Institutional Animal Care and Use Committee in accordance with the National Institutes of Health guidelines.

Abs and reagents

The following Abs were used for immunohistochemistry: Armenian hamster anti-mouse CD11c (clone HL3; BD Biosciences), rat anti-mouse Gr1 (clone RB6-8C5; BD Biosciences), rat anti-mouse F4/80 (clone Cl:A3-1; AbD Serotec), rat anti-mouse CD16/32 (clone 93; eBioscience), rabbit polyclonal anti-mouse GM-CSFRα (M-20; Santa Cruz), rat anti-mouse GM-CSFRβ (clone RM0112-42A7; Abcam), rat anti-mouse GM-CSF (clone 4H94, sc-71165; Santa Cruz), rabbit polyclonal anti-mouse Ki67 (ab15580; Abcam), sheep polyclonal anti-mouse RegIIIβ (cat. no. AF5110; R&D Systems), and rabbit anti-mouse RegIIIγ (provided by Dr. L. Hooper, University of Texas Southwestern Medical Center, Dallas, TX). Secondary IgG Abs used were Cy3-conjugated goat anti-Armenian hamster, goat anti-rat, donkey anti-rat, donkey anti-sheep, biotin-conjugated donkey anti-rat, and DyLight549-conjugated donkey anti-rabbit (Jackson ImmunoResearch). Rat, hamster, and sheep IgG (Jackson ImmunoResearch) and Universal Rabbit Negative Control (DAKO) were used as negative controls.

The following Abs were used for flow cytometry: Alexa Fluor 647–conjugated Armenian hamster anti-mouse CD11c (clone N418; eBioscience), PerCP-Cy5.5–conjugated rat anti-mouse CD11b (clone M1/70; eBioscience), PE-Cy7–conjugated rat anti-mouse B220 (clone RA3-6B2; eBioscience), and FITC-conjugated Armenian hamster anti-mouse CD103 (clone 2E7; eBioscience). The following Abs were used for immunoblot analysis: rabbit polyclonal anti-mouse GM-CSFRα (M-20; Santa Cruz), rabbit polyclonal anti-mouse GM-CSFRβ (Abcam), and mouse anti–β-actin (Sigma-Aldrich). Secondary detection Abs were IRDye800-conjugated goat anti-rabbit and IRDye680–goat anti-mouse (LI-COR Odyssey). Pegylated recombinant mouse GM-CSF (mGM-CSF) was provided by Dr. E. Croze (Bayer HealthCare, Richmond, CA).

DSS-induced colitis

Colitis was induced by allowing mice to drink 1.5–3% (w/v) DSS (m.w. 36,000–50,000; MP Biomedicals) dissolved in the drinking water ad libitum for 6 d. This was followed by a recovery period with no DSS for up to 6 d. Control mice received no DSS throughout the study period. Body weight was monitored daily, and stool samples were tested for occult blood at the indicated times using the Hemoccult test (Beckman Coulter). The bleeding score was determined as follows: negative (no blood) = 0, positive = 1, visible gross blood = 2. Mice were sacrificed after CO_2 inhalation; colons were excised from the cecum to the pelvic brim. Colons were divided longitudinally and used for RNA isolation, protein extraction, histology, and immunohistochemistry. In mice receiving pegylated recombinant mGM-CSF, 5 μg/mouse/d was injected i.p. at the indicated times. Mice injected with PBS were used as controls.

Colon organ culture and ELISA

For explant cultures, the colon was washed in ice-cold PBS supplemented with penicillin (100 U/ml), streptomycin (100 μg/ml), and gentamicin (100 μg/ml), after which the distal colon was cut into 1-cm^2 segments and placed into 12-well plates containing 500 μl RPMI 1640 (Sigma-Aldrich) supplemented with penicillin, streptomycin, and gentamicin, and incubated for 24 h at 37°C, 5% CO_2. Supernatants were centrifuged to remove debris and stored at −80°C until analysis. The remaining tissue pieces were dried and weighed. Cytokine levels in the supernatants were determined by ELISA. Assay sensitivities were 7.8 pg/ml for mGM-CSF, 5 pg/ml for IL-17A, and 3.2 pg/ml for IL-22 (R&D Systems). Data are presented as pg/ml supernatant per gram of explant. For mouse myeloperoxidase (MPO) measurement, pieces of colon were homogenized in lysis buffer (50 mM Tris-HCl, 1% Nonidet P-40, 150 mM NaCl, 1 μg/ml leupeptin, 1 mM PMSF, and 5 mM $NaVO_4$ [pH 8]), and centrifuged twice for 15 min at 15,000 rpm, 4°C. MPO levels were determined by ELISA (Hycult Biotechnology), and concentrations were corrected for tissue protein concentration determined by Bradford assay (Bio-Rad).

Histological analysis and immunohistochemistry

Colons were processed as Swiss rolls (23). Tissues fixed in 10% phosphate-buffered formalin were infused with paraffin using standard tissue processing. Sections of 5 μm were cut and stained with H&E. The length of epithelial ulceration was determined by image analysis of digital photomicrographs of stained sections using the imaging software PictureFrame (Optronics).

For BrdU staining, mice were injected i.p. with 2 mg/mouse BrdU (BD Biosciences) 4 h before sacrifice. Paraffin-embedded colon sections were stained using a BrdU *In-Situ* Detection Kit (BD Pharmingen). To quantify IEC proliferation by BrdU labeling index, we calculated the percentage of BrdU$^+$ cells in 10 well-oriented crypts of each area (nonulcer region or ulcer border) per colon section. TUNEL staining of colon tissue used the ApopTag Peroxidase In Situ Apoptosis Detection Kit (Millipore). Secondary Ab from the kit was replaced by DyLight 488–conjugated monoclonal mouse IgG anti-digoxigenin Ab (Jackson ImmunoResearch). The number of TUNEL$^+$ cells in 15–18 high-power fields (hpfs, 400×) of each colon section was quantified.

For immunohistochemistry, tissues were frozen in optimal cutting temperature compound, and 5-μm sections were fixed in 10% neutral buffered formalin for 10 min, washed, and blocked with 3% BSA in PBS. Sections were incubated with primary Ab (described above) overnight at the following dilutions: anti-mouse CD11c (1:500), F4/80 (1:3000), Gr1 (1:50), RegIIIβ (1:250), RegIIIγ (1:250), and GM-CSFRβ (1:500); this was followed by a 2-h incubation with secondary Abs. Secondary Abs were Cy3-conjugated goat anti-Armenian hamster (1:200), goat anti-rat (1:1000), donkey anti-sheep (1:400), donkey anti-rat (1:700), and DyLight 549–conjugated donkey anti-rabbit (1:500). F-actin and nuclei were stained with Alexa Fluor 488–conjugated phalloidin and Hoechst 33342, respectively. For GM-CSF staining, sections were blocked with 0.3% H_2O_2, followed by normal donkey serum (Jackson ImmunoResearch). Sections were incubated with GM-CSF Ab (1:50) overnight, followed by avidin-biotin blocking (Vector Laboratories). Biotin-conjugated donkey anti-rat secondary Ab (1:500) was added for 2 h, followed by HRP-conjugated streptavidin (1:700; Jackson ImmunoResearch) and incubation with 3,3′-diaminobenzidine (Vector Laboratories).

For GM-CSFRα staining, 5-μm paraffin sections were deparaffinized in xylene and hydrated. Sections were then blocked with 3% BSA in PBS, followed by CD16/32 for FcR blocking. Heat-induced Ag retrieval was performed with citrate buffer (pH 6). Anti-mouse GM-CSFRα Ab (1:500) was applied for 24 h, followed by 2 h of incubation with Cy3-conjugated donkey anti-rabbit Ab (1:400). The Ig fraction of serum from nonimmunized rabbits was used as a negative control.

Samples were examined in our laboratory under an Olympus BX41 microscope or a Hamamatsu NanoZoomer 2.0HT slide scanning system at the University of California, San Diego Neuroscience Microscopy Shared Facility. Digital images were processed using Adobe Photoshop 9.0 (Adobe Systems), with the same settings being applied for test and control Ab.

Immunoblot analysis for GM-CSFR components

Isolated crypts were homogenized in RIPA buffer (Santa Cruz) supplemented with a mixture of protease inhibitors, PMSF, and sodium orthovanadate (as per the manufacturer's instructions). Lysates were separated on a 12% polyacrylamide Mini-PROTEAN TGX Precast Gel, and proteins were transferred to polyvinylidene fluoride membranes (Whatman). Membranes were blocked with buffer containing 5% skim milk for 1 h at room temperature and probed with primary Abs GM-CSFRα (1:500), GM-

CSFRβ (1:500), and β-actin (1:5,000) overnight at 4˚C, followed by incubation with secondary detection Abs (1:10,000) for 2 h at room temperature. Membranes were washed in PBS and scanned for infrared signal using the Odyssey Imaging System (LI-COR Biosciences). Lysates from the murine monocyte/macrophage cell line RAW246.7 were used as a positive control.

Lymphocyte isolation from colon lamina propria

Colons were removed, cut longitudinally, and washed with ice-cold PBS. To remove epithelial cells, colons were cut into 5-mm pieces and incubated for 20 min in predigestion solution (HBSS containing 5 mM EDTA, 10 mM HEPES, 1 mM DTT supplemented with penicillin, streptomycin, and gentamicin) at 37˚C with agitation. After incubation, samples were shaken vigorously, supernatant was removed, and fresh predigestion solution was added to the tissue. After repeating this procedure three times and discarding supernatants containing epithelial cells, tissues were washed, minced, and digested in DMEM containing 10% FCS, 0.5 mg/ml Collagenase D (Roche), and 0.1 mg/ml DNase (Roche) supplemented with penicillin, streptomycin, and gentamicin for 20 min at 37˚C with gentle agitation. Digested tissues were passed through a 40-μm cell strainer, and cells were washed, counted, and used for flow cytometry.

Flow cytometry

For multicolor flow cytometry, isolated cells were suspended in PBS containing 1% FBS, 2 mM EDTA (FACS buffer) and incubated with 0.5 μg anti-mouse CD16/32 for 30 min at 4˚C to block FcRs. After blocking, surface staining was performed for 30 min at 4˚C in the dark with the corresponding mixture of fluorescently labeled Abs. Cells were washed twice, resuspended in FACS buffer, and fixed with 2% paraformaldehyde. The LIVE/DEAD Fixable Aqua Dead Cell Stain Kit (Invitrogen) was used to determine cell viability. Data were acquired on a BD FACSAria II instrument, and analysis was performed using FACSDiva software (BD Biosciences) at the Flow Cytometry Research Core Facility (VA San Diego Healthcare System, San Diego, CA).

RNA extraction and real-time RT-PCR

Whole colon was washed in PBS and cut into 3–5-mm pieces. Total RNA was extracted using a RNeasy Mini Kit (QIAGEN), and DNA was eliminated with DNase (QIAGEN). Reverse transcription used the ImProm-II Reverse Transcription System (Promega). Quantitative real-time RT-PCR amplification was performed on a StepOnePlus Real-Time PCR System (Applied Biosystems) using SYBR Green PCR Master Mix (Applied Biosystems). Mouse primers are listed in Table I. The expression of each mRNA was normalized to GAPDH expression and compared with the mRNA levels of untreated mice.

Isolation of mouse colon crypts

Colons were cut longitudinally, and feces were removed by washing with PBS. Colons cut into 2–3-mm pieces were gently rocked for 10 min at 37˚C in HBSS containing 30 mM EDTA supplemented with penicillin, streptomycin, and gentamicin. After supernatant was removed, ice-cold PBS was added to the tissue pieces, which were vigorously shaken to liberate the crypts. For separating crypts (i.e., epithelial cells) from contaminating nonepithelial cells, the supernatant suspension was allowed to sediment for 15 min at 4˚C. The sedimented cells (mostly complete crypts) were collected and washed with PBS. Crypt IECs were positive for cytokeratin staining. Contamination by $CD3^+$ T cells was <2%.

Expression array profiling

Total RNA (isolated by RNeasy kit; QIAGEN) was prepared from isolated crypts of WT and GM-$CSF^{-/-}$ mice colons before or after 1.5% DSS treatment for 6 d. Purified RNA (150 ng/sample) was labeled using the Low Input Quick Amp Labeling Kit One-Color and then hybridized to a mouse whole-genome microarray 4 × 44K 60-mer slides, according to the manufacturer's instructions (Agilent). Three biological replicates were performed for each experimental condition. Expression values were normalized using a multiple-loess method (24). Based on the histogram of $\log_2$-transformed values, a probe was scored as detected if its signal intensity exceeded 75 in at least one sample, which resulted in 34,235

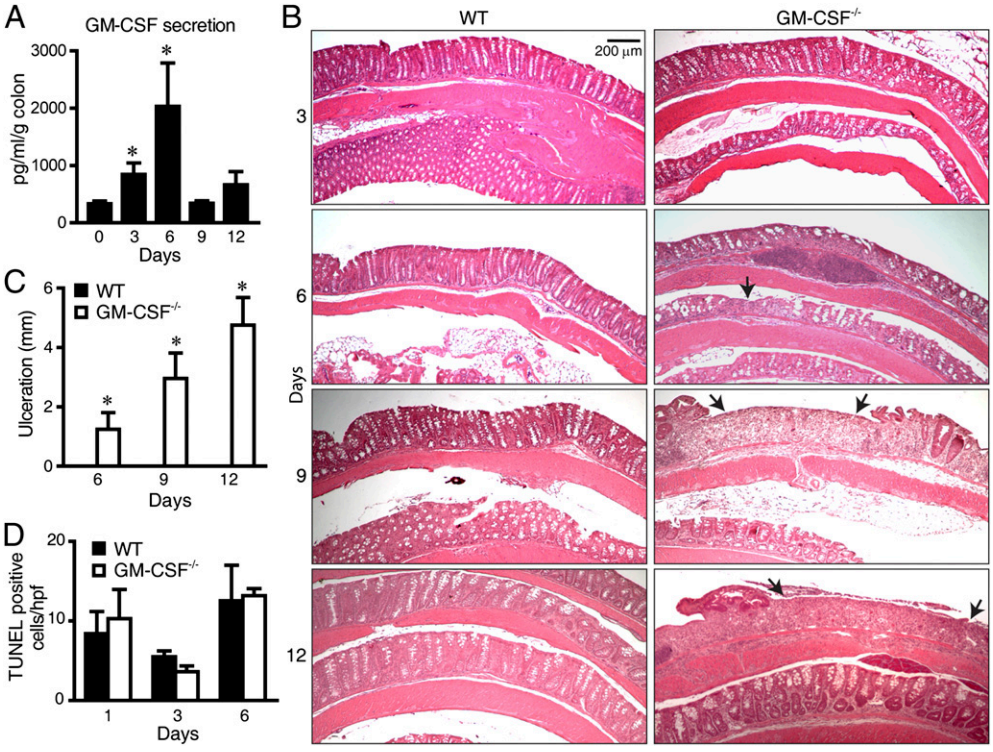

FIGURE 1. GM-CSF enhances mucosal regeneration in DSS-induced colitis. (**A**) GM-CSF protein was measured by ELISA in supernatants of colon explants from WT mice treated with 1.5% DSS. Data are expressed as pg/ml of GM-CSF in supernatant per gram of colon explant tissue. Data are mean ± SEM (n = 3–7 mice/group at each time point). Similar results were obtained in two repeated experiments. *$p < 0.05$, versus day 0. (**B**) H&E-stained sections of mid and distal colon obtained at the indicated time points from WT and GM-$CSF^{-/-}$ mice treated with 1.5% DSS. Arrows indicate areas of ulceration. (**C**) Total ulceration per mouse colon was determined morphometrically (n = 5–9 mice/group at each time point). Similar results were obtained in three repeated experiments. *$p < 0.05$, versus WT mice. (**D**) TUNEL staining of colon sections of WT and GM-$CSF^{-/-}$ mice during treatment with 1.5% DSS for 6 d. Data are mean ± SEM (n = 3–6 mice/group). Similar results were obtained in two repeated experiments.

detected probes used for the subsequent analysis. For the purposes of the false discovery rate (FDR) calculation, control and treatment samples were paired into three control–treatment pairs for each biological comparison. Genes were ranked for each pair according to the $\log_2$ ratio of expression levels, and the rank-sum statistic was calculated. FDR for each gene was calculated as the fraction of genes in the null model (defined as having uncorrelated ranks among the replicates) whose rank-sum statistic was as or more extreme than the observed one. Genes were then sorted and ranked according to their FDR. Genes involved in at least one of the three gene ontology (GO) processes—"cell cycle," "regulation of cell proliferation," and "response to wounding"—that were differentially regulated at least ± 2.5-fold in DSS–GM-CSF$^{-/-}$ mice versus DSS-WT mice were subsequently clustered; their expression patterns were displayed as a heat map. Red indicates increased expression and blue indicates decreased expression relative to the median transcript expression. Datasets are available under accession number GSE42173 from the National Center for Biotechnology Information/Gene Expression Omnibus (http://www.ncbi.nlm.nih.gov/geo/query/acc.cgi?acc=GSE42173).

DC depletion

For depletion of CD11c$^+$ DCs, mice expressing the diphtheria toxin receptor (DTR) on CD11c$^+$ cells (DTR mice) (25) were treated with 4 ng/g diphtheria toxin (DTX) i.p. (Sigma Aldrich) on day 3 of DSS (1.5%) treatment. Depletion of CD11c$^+$ DCs in the colon mucosa was confirmed by immunostaining on day 6, as described previously (26).

BM chimeras

To generate BM chimeric mice, 6–10-wk-old WT, GM-CSF$^{-/-}$, and GM-CSFRβc$^{-/-}$ recipients received a single lethal dose of 9 Gy total body irradiation from a [^{137}Cs] source. Eight hours later, mice were injected i.v. with 2–5 × 10^6 BM cells from sex-matched WT, GM-CSF$^{-/-}$, or GM-CSFRβc$^{-/-}$ donor mice and then rested for 8 wk before use. Chimerism was confirmed by PCR analysis of DNA from peripheral blood cells and auricular appendages.

Statistical analyses

Differences between samples were evaluated by the Mann–Whitney rank-sum test or the Student *t* test for comparing two groups; ANOVA was used for multiple-group comparisons. The Tukey post hoc test was used for multiple pair-wise comparisons. Values are expressed as mean ± SEM. The p values < 0.05 were considered significant.

Results

GM-CSF$^{-/-}$ mice develop more severe DSS-induced colitis than WT mice

To probe the role of GM-CSF in facilitating recovery of the colon epithelium after injury, we used gene-targeted mice deficient in GM-CSF. DSS at concentrations ≥3% is often used to induce murine colitis and results in significant mucosal ulceration and inflammation in WT mice, a finding that we confirmed. Although WT mice eventually recovered from 3% DSS, this concentration was uniformly lethal in GM-CSF$^{-/-}$ mice, causing extensive epithelial denudation and ulceration, as well as weight loss and fecal blood loss that persisted after DSS was discontinued (data not shown).

To determine the mechanisms by which endogenous GM-CSF facilitates recovery from DSS-mediated injury, we used a concentration of 1.5% DSS in the drinking water. DSS (1.5%) increased GM-CSF production in the colons of WT mice (Fig. 1A), and these mice developed few, if any, ulcers (Fig. 1B, *left panels*, 1C). In contrast, GM-CSF$^{-/-}$ mice developed marked mucosal erosions and ulcers (Fig. 1B, *right panels*, 1C), but all mice ultimately recovered after DSS was discontinued.

Increased epithelial erosions and ulceration in mice lacking GM-CSF relative to WT mice after DSS treatment might reflect greater epithelial cell injury and cell loss mediated by increased apoptosis or, alternatively, the inability of intestinal crypts to replace damaged epithelial cells as efficiently in mice lacking GM-CSF. As assessed by TUNEL staining of IECs on days 1, 3, and 6 of DSS treatment, epithelial apoptosis did not differ significantly between WT and GM-CSF$^{-/-}$ mice (Fig. 1D), indicating that the lack of GM-CSF did not increase IEC death after DSS treatment.

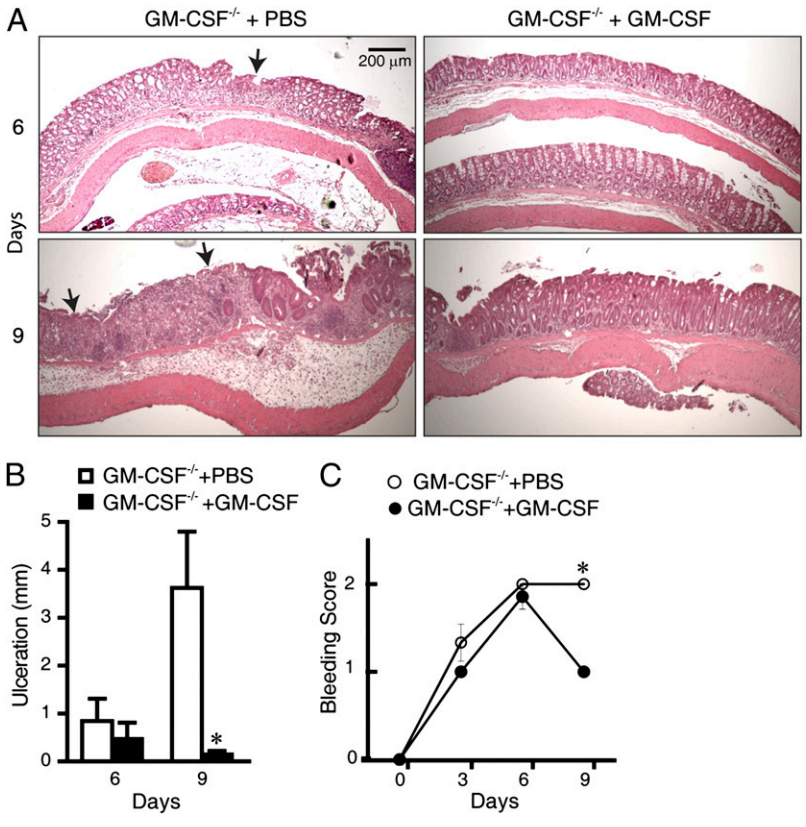

FIGURE 2. GM-CSF administration decreases ulceratio in GM-CSF$^{-/-}$ mice. (**A**) GM-CSF$^{-/-}$ mice administered 1.5% DSS were injected daily with recombinant mGM-CSF (5 μg/mouse) or PBS i.p. from days 1 through 8. Mice were sacrificed on day 6 or 9, and mid and distal colon sections were stained with H&E. Arrows indicate areas of ulceration. (**B**) Total ulceration per mouse colon was determined morphometrically. Data are mean ± SEM (n = 3–5 mice/group at each time point). Similar results were obtained in two repeated experiments. *$p < 0.05$, versus PBS-treated mice. (**C**) Bleeding scores were measured by Hemoccult test using the following scoring system: no blood = 0, positive = 1, visible gross blood = 2. Data are mean ± SEM (n = 3–6 mice/group at each time point). Similar results were obtained in two repeated experiments. *$p < 0.05$, versus PBS-injected GM-CSF$^{-/-}$ mice.

To exclude the possibility that GM-CSF$^{-/-}$ mice had a developmental abnormality that altered the regenerative capacity of the injured intestinal epithelium, we administered mGM-CSF to DSS-treated GM-CSF$^{-/-}$ mice. GM-CSF$^{-/-}$ mice receiving exogenous mGM-CSF had a significant decrease in colon ulceration (Fig. 2A, 2B) and bleeding score (Fig. 2C) compared with mice receiving PBS. Thus, the impaired mucosal repair in GM-CSF$^{-/-}$ mice was specifically due to a lack of GM-CSF and not another developmental deficiency in the GM-CSF$^{-/-}$ mice.

Our analysis showed that GM-CSFRβc$^{-/-}$ mice, which lack the signaling β-chain of the GM-CSFR, also developed greater mucosal injury and colon ulceration from day 6 through 12 after 1.5% DSS compared with WT mice (Supplemental Fig. 1A). These findings indicated that GM-CSF signaling through its receptor has

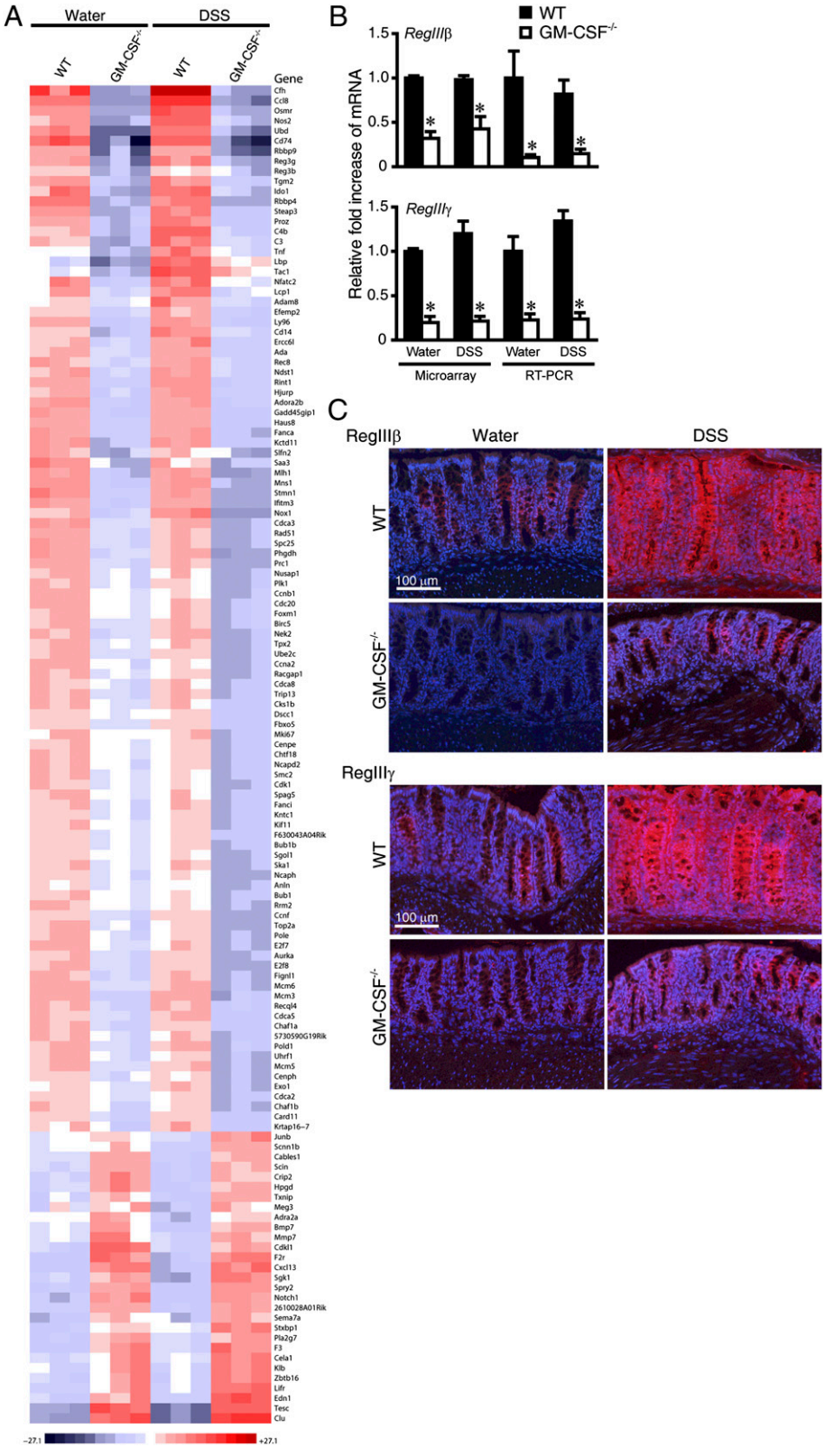

FIGURE 3. Expression profile of genes involved in cell cycle, cell proliferation, and/or wound response in colonic crypts. (**A**) WT and GM-CSF$^{-/-}$ mice were administered 1.5% DSS in water or water alone for 6 d, and colonic crypts were isolated. RNA was extracted from cohorts of three mice/group (each column represents one mouse) and subjected to gene-expression profiling using whole-genome oligonucleotide arrays (Agilent). Genes expressed at least ±2.5-fold in DSS–GM-CSF$^{-/-}$ mice compared with DSS-WT mice with an FDR < 0.05 are represented and clustered according to their expression patterns. The heat map shows relative expression per gene per sample with respect to the median value across all samples for each gene. Downregulated genes are represented in blue; upregulated genes are represented in red. (**B**) *RegIIIβ* and *RegIIIγ* microarray expression data were confirmed by RT-PCR in isolated colonic crypts. Data are mean ± SEM (n = 3 mice/group). (**C**) RegIIIβ and RegIIIγ protein expression (shown in red) was verified by immunohistochemistry in colon sections from WT and GM-CSF$^{-/-}$ mice before and after 6 d of DSS treatment. Nuclei are shown in blue. Similar results were obtained in three repeated experiments. Scale bar, 100 μm. *$p < 0.05$, versus WT mice.

an important role in protection of the colon mucosa from DSS-induced epithelial injury.

Gene-expression analysis of colon crypt epithelial cells in unchallenged and DSS-challenged GM-CSF$^{-/-}$ and WT mice

Epithelial regeneration in the colon is initiated in the crypts (27). To discover possible molecular mechanisms mediated by GM-CSF that may be involved in regeneration of the colon epithelium after DSS-induced injury, we performed whole genome–wide mRNA microarray analysis of isolated crypt epithelial cells from unchallenged and DSS-challenged WT and GM-CSF$^{-/-}$ mice. Crypts were isolated from control mice and DSS-challenged mice 6 d after DSS administration, because that time preceded the severe crypt loss in GM-CSF$^{-/-}$ mice. Of 44,000 expression tags analyzed, 260 were significantly downregulated and 217 were upregulated with a fold change greater than ± 2.5 in unchallenged GM-CSF$^{-/-}$ mice compared with WT mice. After DSS treatment, 400 expression tags were downregulated and 296 were upregulated in DSS-treated GM-CSF$^{-/-}$ mice compared with DSS-treated WT mice. GO analysis of the downregulated and upregulated genes showed that biological processes with the GO terms "cell cycle," "regulation of cell proliferation," and "response to wounding" were differentially regulated in WT and GM-CSF$^{-/-}$ crypts. After DSS treatment of GM-CSF$^{-/-}$ and WT mice, 108 expression tags involved in these biological processes were significantly downregulated and 29 were upregulated $\geq$2.5-fold in GM-CSF$^{-/-}$ mice compared with crypts of WT mice (shown as a heat map in Fig. 3A, Supplemental Table I). Reduced expression of some of these genes known to be important for tissue repair and regeneration, IEC proliferation, or epithelial wound healing (e.g., *RegIIIβ* and *RegIIIγ*) (28–30) was confirmed by real-time RT-PCR and immunohistochemistry (Fig. 3B, 3C, Table I).

Decreased crypt epithelial cell proliferation after DSS in GM-CSF$^{-/-}$ mice

To determine whether the altered expression levels of genes involved in "cell cycle," "regulation of cell proliferation," and "response to wounding" in GM-CSF$^{-/-}$ crypts were paralleled by a functional decrease in IEC proliferation in vivo, we assessed IEC proliferation by BrdU staining in GM-CSF$^{-/-}$ and WT mice over 6 d of 1.5% DSS treatment and the ensuing 6-d recovery period. Proliferation of IECs, as assessed by BrdU staining, was significantly decreased in both WT and GM-CSF$^{-/-}$ mice by 1 d after DSS treatment (Fig. 4Ac, 4Ad, 4B). IEC proliferation recovered by day 3 of DSS treatment in WT crypts, but recovery in the crypts of GM-CSF$^{-/-}$ mice was not apparent until day 9 (i.e., 3 d after DSS was discontinued) (Fig. 4Ae–j, 4B). IEC proliferation was similar in nonulcerated regions of WT and GM-CSF$^{-/-}$ mice from days 9 to 12 but was significantly greater in the areas bordering the ulcers in GM-CSF$^{-/-}$ mice (Fig. 4Ai–n, 4B). Similar results were seen in DSS-treated GM-CSFRβc$^{-/-}$ mice (Supplemental Fig. 1B, 1C) and with Ki67 staining (data not shown). Moreover, administration of recombinant mGM-CSF to DSS-treated GM-CSF$^{-/-}$ mice significantly increased the numbers of proliferating crypt cells (Fig. 4C, 4D). These results revealed that decreased proliferation of IECs in the colon crypt compartment that occurs after mucosal injury in mice lacking GM-CSF can be corrected by exogenous GM-CSF. In contrast, mGM-CSF administration in WT mice in the absence of DSS treatment did not significantly increase colon crypt cell proliferation (Fig. 4E, 4F). This suggested that increased IEC proliferation that occurs in response to GM-CSF release might require GM-CSF acting in combination with other mediators or processes activated by mucosal injury.

TNF was reported to stimulate GM-CSF production in alveolar epithelial cells in vitro and appeared to have a key role in alveolar epithelial cell proliferation and the production of GM-CSF in bronchoalveolar lavage fluid in an in vivo model of LPS-induced lung injury (22). TNF stimulation also was reported to increase GM-CSF mRNA levels in human colon cancer cell lines (31). To determine whether mucosal GM-CSF production after DSS injury was TNF dependent, we assessed mucosal GM-CSF production after DSS administration for 6 d in WT and TNF-deficient (TNFα$^{-/-}$) mice. However, we found no significant difference in mucosal GM-CSF secretion or the magnitude of colon epithelial cell proliferation after

Table I. Oligonucleotide primers used in this study

Primer		Sequence 5′–3′
GM-CSF exon 3	Sense	5′-ACTCCGGAAACGGACTGTGAAACA-3′
	Antisense	5′-AGCAGCAGTCTGAGAAGCTGGATT-3′
GAPDH	Sense	5′-CGATGCCCCCATGTTTGTGAT-3′
	Antisense	5′-GGTCATGAGCCCTTCCACAATGC-3′
CSF1	Sense	5′-GACTTCATGCCAGATTGCC-3′
	Antisense	5′-GGTGGCTTTAGGGTACAGG-3′
CCL2	Sense	5′-TTGACCCGTAAATCTGAAGC-3′
	Antisense	5′-CGAGTCACACTAGTTCACTG-3′
CXCL1	Sense	5′-GCCAATGAGCTGCGCTGT-3′
	Antisense	5′-CCTTCAAGCTCTGGATGTTCTT-3′
CXCL2	Sense	5′-ATCCAGAGCTTGAGTGTGACGC-3′
	Antisense	5′-AAGGCAAACTTTTTGACCGCC-3′
IL-6	Sense	5′-ACAACCACGGCCTTCCCTAC-3′
	Antisense	5′-ACAATCAGAATTGCCATTGCAC-3′
IL-17A	Sense	5′-CAGGACGCGCAAACATGA-3′
	Antisense	5′-GCAACAGCATCAGAGACACAGAT-3′
Reg3β	Sense	5′-CAGACCTGGTTTGATGCAGA-3′
	Antisense	5′-GAAGCCTCAGCGCTATTGAG-3′
Reg3γ	Sense	5′-ATGGCTCCTATTGCTATGCC-3′
	Antisense	5′-GATGTCCTGAGGGCCTCTT-3′
GM-CSFRα	Sense	5′-GTGACGCGCCGACTCTT-3′
	Antisense	5′-GGGGCTATAGAGGAGGATTTG-3′
GM-CSFRβ	Sense	5′-GTAAGATGAGTGGAGCCAAACC-3′
	Antisense	5′-CCGTTTCTTCTGCCTCTGTC-3′
IL-22	Sense	5′-TCCGAGGAGTCAGTGCTAAA-3′
	Antisense	5′-AGAACGTCTTCCAGGGTGAA-3′

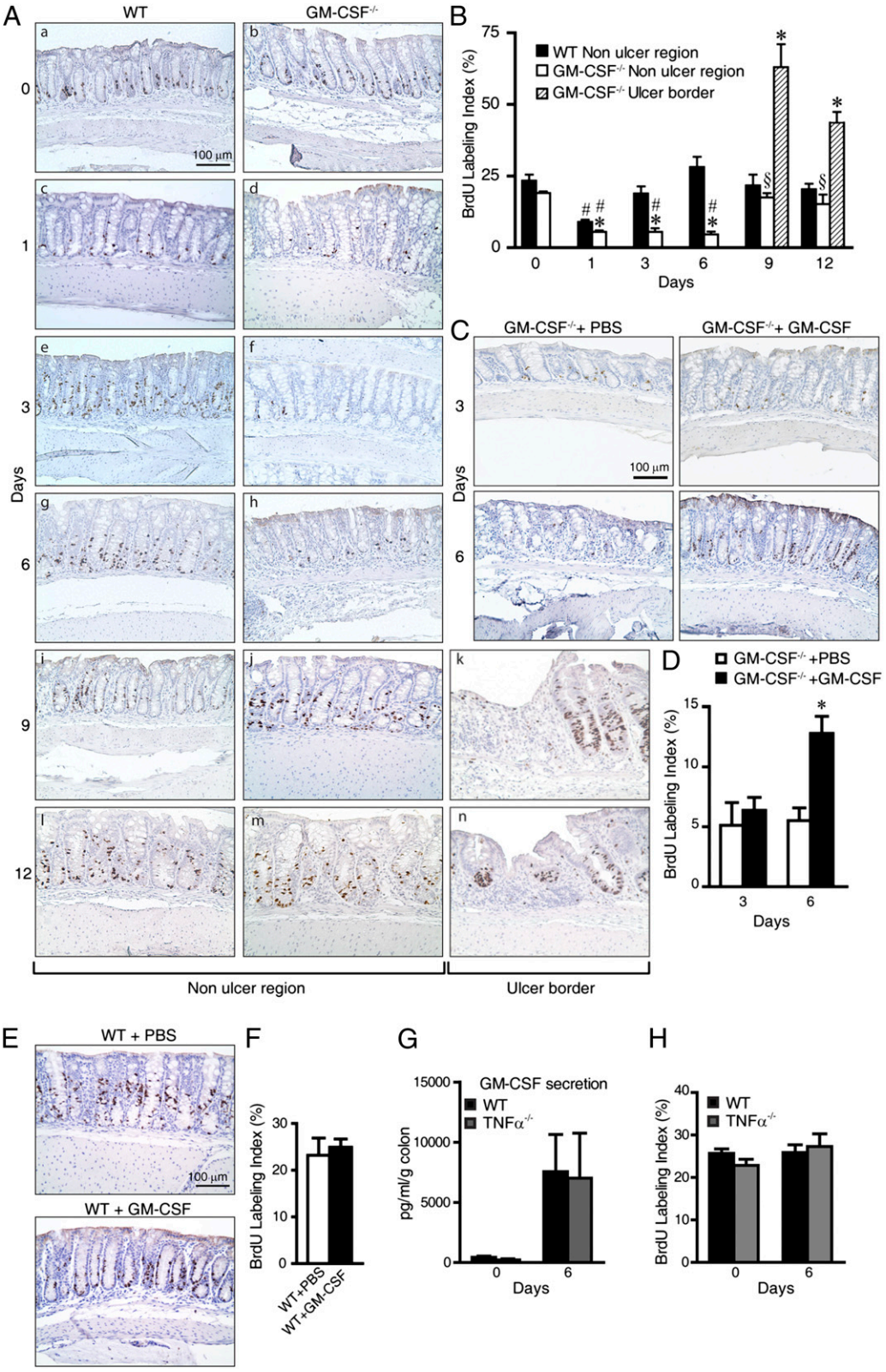

FIGURE 4. Epithelial cell proliferation in DSS-treated GM-CSF$^{-/-}$, TNFα$^{-/-}$, and WT mice. (**Aa**–**n**) BrdU staining (dark brown) in colon sections of WT and GM-CSF$^{-/-}$ mice before and after 1.5% DSS treatment (6 d of DSS followed by 6 d of recovery). Scale bar, 100 μm. (**B**) Quantification of BrdU staining shown as BrdU labeling index (percentage of proliferating cells/crypt) at the indicated time points. Data are mean ± SEM (n = 3–6 mice/group). Similar results were obtained in two repeated experiments. *$p < 0.05$, versus WT mice, $^{\#}p < 0.05$, versus WT or GM-CSF$^{-/-}$ mice not treated with DSS, $^{\S}p < 0.05$, versus GM-CSF$^{-/-}$ mice at day 6. (**C**) BrdU staining in colon sections of GM-CSF$^{-/-}$ mice injected i.p. with PBS or recombinant mGM-CSF for 3 or 6 d during 1.5% DSS treatment. Scale bar, 100 μm. (**D**) BrdU staining at the indicated time points of GM-CSF$^{-/-}$ mice receiving PBS or mGM-CSF after 1.5% DSS treatment was quantified as BrdU labeling index. Data are mean ± SEM (n = 3–5 mice/group). Similar results were obtained in two repeated experiments. *$p < 0.05$, versus PBS-injected mice. (**E**) BrdU staining of colon sections from WT mice injected i.p. with PBS or 5 μg recombinant mGM-CSF/day for 3 d. Scale bar, 100 μm. (**F**) BrdU labeling index in WT mice injected with PBS or recombinant mGM-CSF as (*Figure legend continues*)

DSS in WT mice compared with TNFα$^{-/-}$ mice (Fig. 4G, 4H), indicating that mucosal GM-CSF production and GM-CSF–dependent epithelial cell proliferation after DSS were not TNF dependent.

Next, we considered the possibility that increased inflammatory mediators in the mucosa of mice lacking GM-CSF may contribute to the decreased crypt IEC proliferation in GM-CSF$^{-/-}$ mice compared with WT mice after DSS treatment. Certain chemokines and cytokines were selectively increased in GM-CSF$^{-/-}$ mice relative to WT mice (*CXCL1*, *CXCL2*, *CCL2*, *IL-6*, *CSF1*), but this occurred at later time points (Fig. 5) when epithelial cell proliferation had also increased (Fig. 4A, 4B). However, they were not upregulated at the time when there was a significant decrease in crypt epithelial cell proliferation in GM-CSF$^{-/-}$ mice treated with DSS. Moreover, cytokines specifically thought to be important in epithelial proliferation and wound healing, e.g., IL-22 (32) and IL-17A (33, 34), did not differ significantly between DSS-treated WT and GM-CSF$^{-/-}$ mice (data not shown), indicating that these mediators are not likely to explain the early increased epithelial cell proliferative response in WT mice.

Taken together, these results indicate an essential and nonredundant role for GM-CSF in promoting epithelial cell proliferation at early times after the initiation of mucosal injury, whereas GM-CSF was not a requisite for epithelial cell proliferation during the later period of recovery from DSS-induced mucosal injury or in the steady state.

Nonhematopoietic cells are the source of GM-CSF important for colon epithelial cell proliferation after DSS injury

To determine whether the source of GM-CSF responsible for crypt epithelial proliferation was derived from cells of hematopoietic or nonhematopoietic origin, we generated BM chimeras. GM-CSF$^{-/-}$ mice reconstituted with WT BM (WT BM→GM-CSF$^{-/-}$) manifested decreased epithelial proliferation and concurrently developed mucosal ulcerations similar to GM-CSF$^{-/-}$ mice after treatment with 2% DSS for 6 d. In contrast, when GM-CSF$^{-/-}$ BM was transferred to WT mice (GM-CSF$^{-/-}$ BM→WT), epithelial cell proliferation and ulceration were similar to that in control WT chimeras (WT BM→WT) with DSS treatment (Fig. 6A–C). These results indicated that GM-CSF produced by cells of nonhematopoietic origin were the source of GM-CSF associated with increased epithelial cell proliferation and decreased mucosal ulceration in WT mice relative to GM-CSF–deficient mice.

Because mouse colon crypt epithelial cells from WT and GM-CSF$^{-/-}$ mice express α- and β-chains of the GM-CSFR, as assessed by RT-PCR, immunoblotting, and immunostaining (Supplemental Fig. 2A–C), we transferred GM-CSFRβc$^{-/-}$ BM into WT recipients (GM-CSFRβc$^{-/-}$BM→WT) and determined that the presence of the GM-CSFR on nonhematopoietic cells was sufficient to restore epithelial cell proliferation after 6 d of DSS treatment (Supplemental Fig. 3). These results further indicated that the effect of GM-CSF on colon epithelial proliferation was, at least in part, driven by cells of nonhematopoietic origin.

To determine which nonhematopoietic cells produced GM-CSF after DSS treatment, colon sections from DSS-treated WT mice were immunostained for GM-CSF. We found that colon epithelial cells, which stained positive for GM-CSF, were the nonhematopoietic cell source of GM-CSF production after DSS treatment (Fig. 6D).

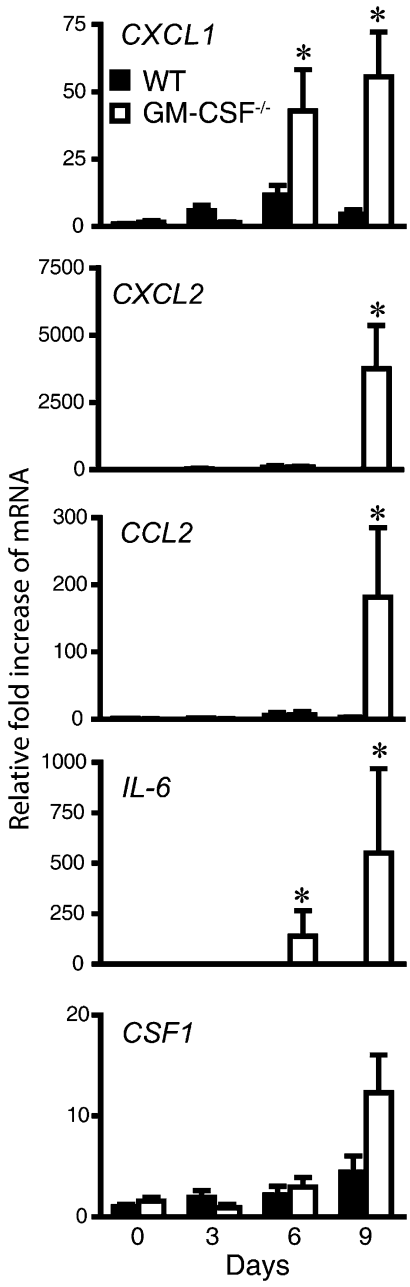

FIGURE 5. Cytokine and chemokine expression in 1.5% DSS–treated GM-CSF$^{-/-}$ mice compared with WT mice. mRNA transcripts for the chemokines *CXCL1*, *CXCL2*, *CCL2* and the cytokines *IL-6* and M-CSF (encoded by *CSF1*) were determined by real-time RT-PCR in the mid and distal colon of WT and GM-CSF$^{-/-}$ mice during the time course of 1.5% DSS treatment (6 d of DSS followed by 3 d of recovery). Data are mean ± SEM (n = 4–8 mice/group at each time point). Similar results were obtained in two repeated experiments. *$p < 0.05$, versus WT mice.

Because previous studies that administered high doses of DSS to GM-CSF$^{-/-}$ mice suggested that cells of hematopoietic origin, such as macrophages (14), neutrophils (21), or splenic DCs (20), may have an important role in the response to GM-CSF in DSS-

in (**E**). Data are mean ± SEM (n = 3–5 mice/group). Similar results were obtained in two repeated experiments. *$p < 0.05$, versus PBS-injected mice. (**G**) GM-CSF protein was measured by ELISA in supernatants of colon explants from WT and TNFα$^{-/-}$ mice treated with 2% DSS at the indicated times. Data are mean ± SEM (n = 3–4 mice/group). Similar results were obtained in two repeated experiments. (**H**) BrdU labeling index in colon sections of WT and TNFα$^{-/-}$ mice treated with 2% DSS at the indicated times. Data are mean ± SEM (n = 4–7 mice/group). Similar results were obtained in two repeated experiments.

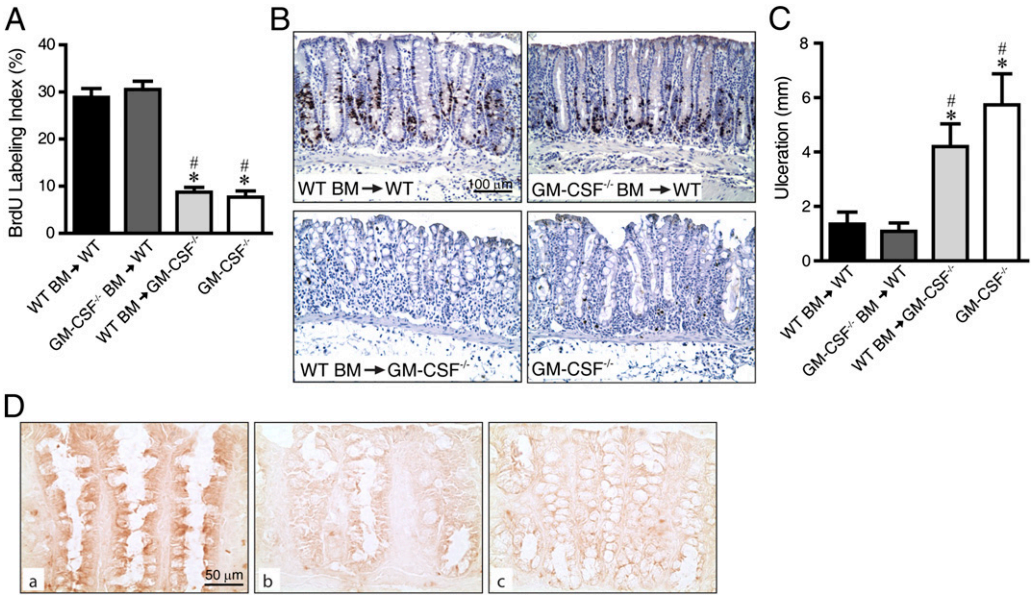

FIGURE 6. GM-CSF production by nonhematopoietic cells increases epithelial cell proliferation and decreases susceptibility to DSS-induced colon ulceration. (**A**) Quantification of BrdU staining shown as BrdU labeling index (percentage of proliferating cells/crypt) (n = 11–14 mice/group). Similar results were obtained in three repeated experiments. (**B**) BrdU staining (dark brown) in colon sections of chimeric mice WT BM→WT, GM-CSF$^{-/-}$ BM→WT, and WT BM→GM-CSF$^{-/-}$ and GM-CSF$^{-/-}$ control mice after 6 d of DSS treatment. Scale bar, 100 μm. (**C**) Total ulceration per mouse colon was determined morphometrically in chimeric mice WT BM→WT, GM-CSF$^{-/-}$ BM→WT, and WT BM→GM-CSF$^{-/-}$ and GM-CSF$^{-/-}$ control mice after 6 d of DSS treatment (n = 11–13 mice/group). Similar results were obtained in three repeated experiments. (**Da**) GM-CSF immunostaining of epithelial cells in colon sections from WT mice treated with 1.5% DSS for 6 d. (**Db**) IgG2a isotype control immunostaining for (Da). (**Dc**) GM-CSF immunostaining in colon sections from GM-CSF$^{-/-}$ mice treated as in (Da). Scale bar, 50 μm. *$p < 0.05$, versus WT BM→WT recipient mice, $^{\#}p < 0.05$, versus GM-CSF$^{-/-}$ BM→WT mice.

colitis, we also assessed these cell types in the colon mucosa. We found no significant difference in the numbers of macrophages (assessed by F4/80$^+$ cells) and neutrophils (assessed by Gr1$^+$ cells and MPO protein levels) between WT and GM-CSF$^{-/-}$ mice after DSS treatment (Fig. 7A–C). Although the numbers of CD11c$^+$ DCs were significantly decreased by ~50% in GM-CSF$^{-/-}$ mice relative to WT mice after DSS (Fig. 7D, 7E), there was no significant difference in the localization of CD11c$^+$ cells after DSS or in the distribution of those cells coexpressing CD11b, CD103, or B220 between WT and GM-CSF$^{-/-}$ mice (data not shown). To determine whether the decreased numbers of CD11c$^+$ DCs in DSS-treated GM-CSF$^{-/-}$ mice were a significant contributor to the increased mucosal ulceration and impaired epithelial cell proliferation in those mice, we depleted CD11c$^+$ DCs from CD11c$^+$-DTR mice (Fig. 7F). The extent of mucosal ulceration and epithelial proliferation were similar in DSS-treated CD11c$^+$ DC–depleted mice (i.e., DTR + DTX) and WT mice, and both were significantly different from DSS-treated GM-CSF$^{-/-}$ mice (Fig. 7G, 7H).

Discussion

Using the well-established DSS model of colonic mucosal injury and inflammation (16, 35) and mice genetically deficient in GM-CSF, we show that GM-CSF has an important functional role in facilitating repair in response to injury of the colon epithelium in vivo. When developing the model, we sought a dose of DSS that consistently caused little, if any, mucosal ulceration and inflammation in WT mice but significant colon ulceration in GM-CSF$^{-/-}$ mice.

We show that endogenous host GM-CSF has a nonredundant role in facilitating epithelial repair at early times after colon epithelial injury. Gene-expression profiling of colon crypts isolated from WT and GM-CSF$^{-/-}$ mice after DSS revealed significant changes in the expression of genes with functions related to the cell cycle, the regulation of cell proliferation, and the response to wounding, with many of the genes in those functional GO groups being significantly downregulated in GM-CSF$^{-/-}$ mice relative to WT mice. Moreover, decreased expression of epithelial genes associated with cell proliferation in GM-CSF$^{-/-}$ mice was paralleled by a failure to increase crypt epithelial cell proliferation after DSS, unlike WT mice. Nonetheless, crypt epithelial cell proliferation was restored toward normal and resembled that in WT mice when we administered exogenous GM-CSF to GM-CSF$^{-/-}$ mice during the course of DSS treatment, which indicated that GM-CSF$^{-/-}$ mice do not have a developmental abnormality responsible for the failure of the crypt epithelium to proliferate in the initial several days after DSS. Although WT mice had little, if any, loss of the epithelial layer, GM-CSF$^{-/-}$ mice manifested increased mucosal ulceration and delayed healing of mucosal ulcers during DSS treatment, possibly resulting in increased mucosal inflammation due to a compromised epithelial barrier. Although GM-CSF was required for crypt epithelial cell proliferation during the initial 6 d of DSS-induced injury, proliferation of the epithelial layer in areas adjacent to mucosal ulcers was independent of GM-CSF by day 9 during the recovery period.

Despite the lack of an intestinal phenotype in untreated GM-CSF$^{-/-}$ mice, we discovered significant differences between WT and GM-CSF$^{-/-}$ mice in the expression levels of many genes associated with cell cycle, proliferation, and wound healing, even before DSS treatment. However, constitutive levels of crypt epithelial cell proliferation did not differ between untreated GM-CSF$^{-/-}$ and WT mice, and exogenous GM-CSF did not increase crypt epithelial cell proliferation in control untreated WT mice, suggesting that GM-CSF is not required for epithelial proliferation in the steady state. Therefore, we postulate that GM-CSF is required to facilitate increased crypt epithelial cell proliferation when mucosal homeostasis is disturbed by epithelial injury. Consistent with the requirement for injury, other investigators showed that exogenous GM-CSF

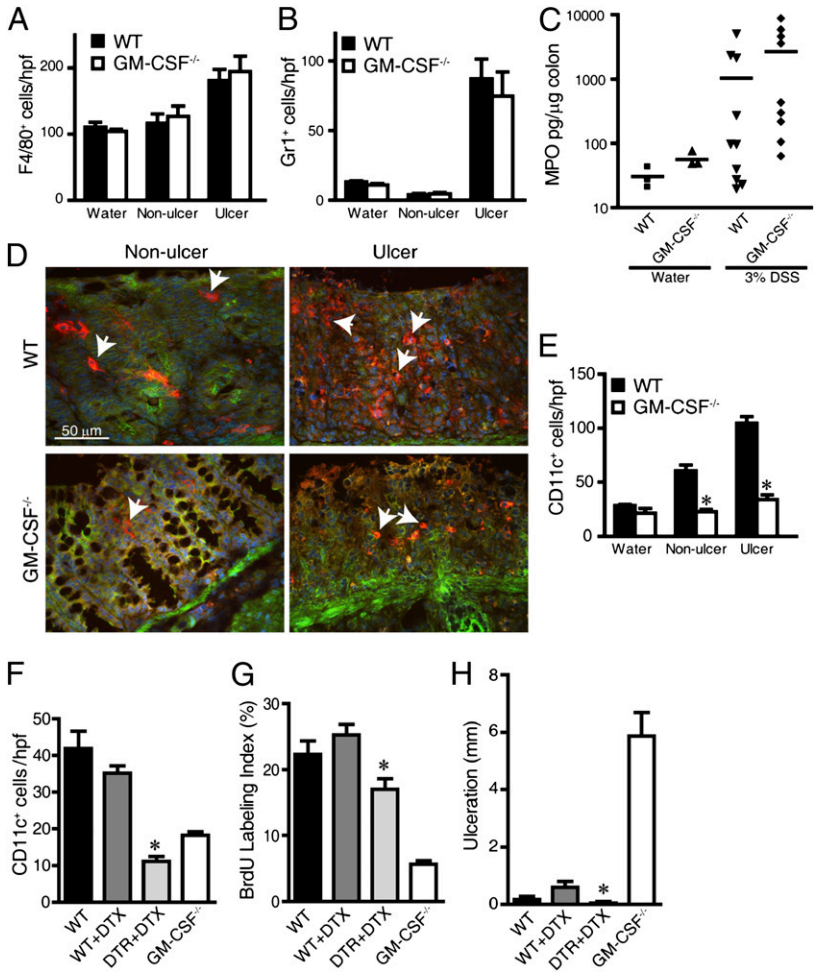

FIGURE 7. Hematopoietic cells, MPO levels, and DC depletion in WT and GM-CSF$^{-/-}$ mice. Number of F4/80$^+$ (**A**) and Gr1$^+$ (**B**) cells in colon sections of WT and GM-CSF$^{-/-}$ mice treated with 3% DSS were quantified on day 9 (6 d of DSS followed by 3 d of recovery) in nonulcerated and ulcerated areas of the colon. Controls received water with no DSS. (**C**) MPO levels measured by ELISA in whole-colon extracts on day 9 and normalized to colon weight (n = 3–10 mice/group). (**D**) Immunostaining of CD11c$^+$ cells in ulcerated and nonulcerated areas of colon sections from WT and GM-CSF$^{-/-}$ mice treated with 3% DSS were assessed on day 9. CD11c$^+$ cells are shown in red (arrows), phalloidin staining of F-actin is shown in green, and nuclei are shown in blue. Scale bar, 50 μm. (**E**) Number of CD11c$^+$ cells in colon sections was determined as in (A, B). Data for (A), (B), and (E) are mean ± SEM of cells/hpf (400×) (n = 4–8 mice/group, n = 5 hpf/group). Number of CD11c$^+$ cells (**F**), BrdU labeling index (**G**), and ulceration (**H**) in colon sections of WT mice, WT mice injected with DTX, DTR mice injected with DTX, and GM-CSF$^{-/-}$ mice were determined at day 6 after 1.5% DSS treatment. Data are mean ± SEM (n = 4–7 mice/group). Similar results were obtained in two repeated experiments. *$p < 0.05$, versus WT and WT+DTX mice (F), *$p < 0.05$, versus GM-CSF$^{-/-}$ mice (G, H).

decreases the severity of colitis and accelerates ulcer healing in DSS-treated WT mice, but they considered that this was likely due to the activity of GM-CSF on dendritic or other myeloid cells (20, 21).

The cellular source of GM-CSF in the injured colon in vivo was an open question. GM-CSF can be produced by a variety of hematopoietic and nonhematopoietic cell types in response to LPS, IL-1, or TNF stimulation in vitro (36, 37). Further, GM-CSF production by IECs and by colon cancer cells (7, 31) in vitro and by small IECs in vivo (15) was reported. Our chimera experiments showed that nonhematopoietic cells were the source of GM-CSF responsible for crypt epithelial cell proliferation and ulcer healing in the first few days after DSS-induced injury, and colon epithelial cells were shown to be the cellular source of the GM-CSF by immunostaining. Although it is possible that colon epithelial cell–derived GM-CSF acts in concert with other mucosal mediators to upregulate epithelial cell proliferation, we note that, in contrast to a lung injury model (22), TNF was not required for mucosal GM-CSF production in the colon in vivo or for epithelial cell proliferation. Consistent with an autocrine/paracrine effect of GM-CSF on colon epithelial cells, BM chimeras in which the GM-CSFRβc was absent on BM-derived cells, but present on nonhematopoietic cells, showed no major difference from WT mice with regard to epithelial proliferation after DSS treatment. Notably, human IECs also express functional GM-CSFRs (19).

An increased severity of colitis was reported in GM-CSF$^{-/-}$ mice after a high dose of DSS (14), similar to what we observed with 3% DSS treatment, but the mechanisms involved were not addressed. Further, improvement in clinical parameters and histology were reported in WT mice administered exogenous GM-CSF as a treatment for colitis induced by high concentrations of DSS (4–5% DSS) (20, 21). Those studies proposed that the numbers or the function of macrophages (14), plasmacytoid DCs (440c$^+$) in the spleen (20), monocytic subsets, or neutrophils (21) might explain the reported findings, but the specific mechanism by which GM-CSF exerted its action was not demonstrated. Notably, we did not find a significant difference in macrophage or neutrophil numbers between WT and GM-CSF–deficient mice after treatment with 3% DSS, which caused marked mucosal damage in WT mice and was lethal for GM-CSF–deficient mice. Although the number of CD11c$^+$ DCs was decreased by ~50% in DSS-treated GM-CSF$^{-/-}$ mice compared with WT mice after either 1.5 or 3% DSS, there were no significant differences in the composition of the different CD11c$^+$ DC subsets (i.e., CD11b$^+$, CD103$^+$, B220$^+$). Further, in marked contrast to GM-CSF$^{-/-}$ mice, epithelial cell proliferation and mucosal healing after DSS treatment were similar in WT and CD11c$^+$ DC–depleted mice.

Our study highlights the importance of fundamental and novel differences in the mechanisms of injury and mucosal healing between the colon and small intestine. After DSS, GM-CSF produced by colon epithelial cells, but not myeloid cells, was required for the epithelial cell proliferative response and early mucosal ulcer healing. This contrasts with reported small intestinal mucosal injury and ileitis caused by the NSAID piroxicam, in which transferred hematopoietic cells significantly ameliorated NSAID injury (15). Although the current study and Han et al. (15) indicated the GM-CSFR on nonhematopoietic cells was required for increased epithelial cell proliferation, the source of GM-CSF that resulted in epithelial proliferation was not addressed in the latter study. Further, we found a similar magnitude of epithelial cell death after

DSS in WT and GM-CSF$^{-/-}$ mice, indicating that GM-CSF did not have a significant role in colon epithelial cell survival, whereas GM-CSF deficiency was associated with increased epithelial cell apoptosis and decreased survival of small IECs after piroxicam (15). A number of possibilities, including those reflecting fundamental differences in the biologic functions mediated by colon and small intestinal mucosa, may explain those differences. In addition, it is known that orally administered DSS results in colon injury but little injury in the small intestine and, unlike the colon epithelium, GM-CSF is produced constitutively by mouse small IECs (5, 15).

In summary, we demonstrate that host GM-CSF produced by colon epithelial cells in response to colon injury has a novel and significant role in decreasing the severity of DSS-induced injury of the colon mucosa by inducing proliferation of crypt epithelial cells. These findings increase our understanding of the role of GM-CSF in mucosal injury and the consequences of a loss of GM-CSF signaling due to a deficiency in GM-CSF, its receptor (38), or the presence of GM-CSF autoantibodies as variably described in some clinical situations (39, 40). Moreover, it is possible that the improvement observed in clinical treatment trials using GM-CSF for inflammatory bowel disease (41–43) may reflect the activity of exogenous GM-CSF on epithelial regeneration under conditions in which the intestinal mucosa is injured.

Acknowledgments

We thank Dr. B. Trapnell for providing GM-CSF$^{-/-}$ and GM-CSFRβc$^{-/-}$ mice, Dr. E. Croze for providing mGM-CSF, and Dr. L. Hooper for providing anti-RegIIIγ Ab. We thank Dr. N. Varki for assistance with immunohistochemistry. The array analysis was carried out at the University of California, San Diego Biomedical Genomics Facility. Microarray data computer analysis was done in consultation with Dr. R. Šášik. We thank J. Norberg, N. Sekiya, and Dr. S. Dann for assistance with flow cytometry and Dr. E. Raz and Dr. L. Eckmann for helpful comments on the manuscript.

Disclosures

The authors have no financial conflicts of interest.

References

1. Hamilton, J. A. 2008. Colony-stimulating factors in inflammation and autoimmunity. *Nat. Rev. Immunol.* 8: 533–544.
2. Martinez-Moczygemba, M., and D. P. Huston. 2003. Biology of common beta receptor-signaling cytokines: IL-3, IL-5, and GM-CSF. *J. Allergy Clin. Immunol.* 112: 653–665, quiz 666.
3. Egea, L., Y. Hirata, and M. F. Kagnoff. 2010. GM-CSF: a role in immune and inflammatory reactions in the intestine. *Expert Rev. Gastroenterol. Hepatol.* 4: 723–731.
4. Sennikov, S. V., V. V. Temchura, V. A. Trufakin, and V. A. Kozlov. 2002. Effects of granulocyte-macrophage colony-stimulating factor produced by intestinal epithelial cells on functional activity of hemopoietic stem cells. *Bull. Exp. Biol. Med.* 134: 548–550.
5. Sennikov, S. V., V. V. Temchura, V. A. Kozlov, and V. A. Trufakin. 2002. The influence of conditioned medium from mouse intestinal epithelial cells on the proliferative activity of crypt cells: role of granulocyte-macrophage colony-stimulating factor. *J. Gastroenterol.* 37: 1048–1051.
6. Fukuzawa, H., M. Sawada, T. Kayahara, Y. Morita-Fujisawa, K. Suzuki, H. Seno, S. Takaishi, and T. Chiba. 2003. Identification of GM-CSF in Paneth cells using single-cell RT-PCR. *Biochem. Biophys. Res. Commun.* 312: 897–902.
7. Hirsch, T., S. Eggstein, S. Frank, E. H. Farthmann, and B. U. von Specht. 1995. Expression of GM-CSF and a functional GM-CSF receptor in the human colon carcinoma cell line SW403. *Biochem. Biophys. Res. Commun.* 217: 138–143.
8. Trutmann, M., L. Terracciano, C. Noppen, J. Kloth, M. Kaspar, R. Peterli, P. Tondelli, C. Schaeffer, P. Zajac, M. Heberer, and G. C. Spagnoli. 1998. GM-CSF gene expression and protein production in human colorectal cancer cell lines and clinical tumor specimens. *Int. J. Cancer* 77: 378–385.
9. Noguchi, M., N. Hiwatashi, Z. X. Liu, and T. Toyota. 2001. Increased secretion of granulocyte-macrophage colony-stimulating factor in mucosal lesions of inflammatory bowel disease. *Digestion* 63(Suppl. 1): 32–36.
10. Ina, K., K. Kusugami, T. Hosokawa, A. Imada, T. Shimizu, T. Yamaguchi, M. Ohsuga, K. Kyokane, T. Sakai, Y. Nishio, et al. 1999. Increased mucosal production of granulocyte colony-stimulating factor is related to a delay in neutrophil apoptosis in Inflammatory Bowel disease. *J. Gastroenterol. Hepatol.* 14: 46–53.
11. Hirata, Y., L. Egea, S. M. Dann, L. Eckmann, and M. F. Kagnoff. 2010. GM-CSF-facilitated dendritic cell recruitment and survival govern the intestinal mucosal response to a mouse enteric bacterial pathogen. *Cell Host Microbe* 7: 151–163.
12. Bogunovic, M., F. Ginhoux, J. Helft, L. Shang, D. Hashimoto, M. Greter, K. Liu, C. Jakubzick, M. A. Ingersoll, M. Leboeuf, et al. 2009. Origin of the lamina propria dendritic cell network. *Immunity* 31: 513–525.
13. Varol, C., A. Vallon-Eberhard, E. Elinav, T. Aychek, Y. Shapira, H. Luche, H. J. Fehling, W. D. Hardt, G. Shakhar, and S. Jung. 2009. Intestinal lamina propria dendritic cell subsets have different origin and functions. *Immunity* 31: 502–512.
14. Xu, Y., N. H. Hunt, and S. Bao. 2008. The role of granulocyte macrophage-colony-stimulating factor in acute intestinal inflammation. *Cell Res.* 18: 1220–1229.
15. Han, X., S. Gilbert, K. Groschwitz, S. Hogan, I. Jurickova, B. Trapnell, C. Samson, and J. Gully. 2010. Loss of GM-CSF signalling in non-haematopoietic cells increases NSAID ileal injury. *Gut* 59: 1066–1078.
16. Okayasu, I., S. Hatakeyama, M. Yamada, T. Ohkusa, Y. Inagaki, and R. Nakaya. 1990. A novel method in the induction of reliable experimental acute and chronic ulcerative colitis in mice. *Gastroenterology* 98: 694–702.
17. Cooper, H. S., S. N. Murthy, R. S. Shah, and D. J. Sedergran. 1993. Clinicopathologic study of dextran sulfate sodium experimental murine colitis. *Lab. Invest.* 69: 238–249.
18. Strober, W., I. J. Fuss, and R. S. Blumberg. 2002. The immunology of mucosal models of inflammation. *Annu. Rev. Immunol.* 20: 495–549.
19. Panja, A., S. Goldberg, L. Eckmann, P. Krishen, and L. Mayer. 1998. The regulation and functional consequence of proinflammatory cytokine binding on human intestinal epithelial cells. *J. Immunol.* 161: 3675–3684.
20. Sainathan, S. K., E. M. Hanna, Q. Gong, K. S. Bishnupuri, Q. Luo, M. Colonna, F. V. White, E. Croze, C. Houchen, S. Anant, and B. K. Dieckgraefe. 2008. Granulocyte macrophage colony-stimulating factor ameliorates DSS-induced experimental colitis. *Inflamm. Bowel Dis.* 14: 88–99.
21. Bernasconi, E., L. Favre, M. H. Maillard, D. Bachmann, C. Pythoud, H. Bouzourene, E. Croze, S. Velichko, J. Parkinson, P. Michetti, and D. Velin. 2010. Granulocyte-macrophage colony-stimulating factor elicits bone marrow-derived cells that promote efficient colonic mucosal healing. *Inflamm. Bowel Dis.* 16: 428–441.
22. Cakarova, L., L. M. Marsh, J. Wilhelm, K. Mayer, F. Grimminger, W. Seeger, J. Lohmeyer, and S. Herold. 2009. Macrophage tumor necrosis factor-alpha induces epithelial expression of granulocyte-macrophage colony-stimulating factor: impact on alveolar epithelial repair. *Am. J. Respir. Crit. Care Med.* 180: 521–532.
23. Maaser, C., M. P. Housley, M. Iimura, J. R. Smith, B. A. Vallance, B. B. Finlay, J. R. Schreiber, N. M. Varki, M. F. Kagnoff, and L. Eckmann. 2004. Clearance of *Citrobacter rodentium* requires B cells but not secretory immunoglobulin A (IgA) or IgM antibodies. *Infect. Immun.* 72: 3315–3324.
24. Sásik, R., C. H. Woelk, and J. Corbeil. 2004. Microarray truths and consequences. *J. Mol. Endocrinol.* 33: 1–9.
25. Jung, S., D. Unutmaz, P. Wong, G. Sano, K. De los Santos, T. Sparwasser, S. Wu, S. Vuthoori, K. Ko, F. Zavala, et al. 2002. In vivo depletion of CD11c+ dendritic cells abrogates priming of CD8+ T cells by exogenous cell-associated antigens. *Immunity* 17: 211–220.
26. McAllister, C. S., O. Lakhdari, G. Pineton de Chambrun, M. G. Gareau, A. Broquet, G. H. Lee, S. Shenouda, L. Eckmann, and M. F. Kagnoff. 2013. TLR3, TRIF, and caspase 8 determine double-stranded RNA-induced epithelial cell death and survival in vivo. *J. Immunol.* 190: 418–427.
27. Medema, J. P., and L. Vermeulen. 2011. Microenvironmental regulation of stem cells in intestinal homeostasis and cancer. *Nature* 474: 318–326.
28. Ogawa, H., K. Fukushima, H. Naito, Y. Funayama, M. Unno, K. Takahashi, T. Kitayama, S. Matsuno, H. Ohtani, S. Takasawa, et al. 2003. Increased expression of HIP/PAP and regenerating gene III in human inflammatory bowel disease and a murine bacterial reconstitution model. *Inflamm. Bowel Dis.* 9: 162–170.
29. Moucadel, V., P. Soubeyran, S. Vasseur, N. J. Dusetti, J. C. Dagorn, and J. L. Iovanna. 2001. Cdx1 promotes cellular growth of epithelial intestinal cells through induction of the secretory protein PAP I. *Eur. J. Cell Biol.* 80: 156–163.
30. Bishnupuri, K. S., Q. Luo, J. R. Korzenik, J. O. Henderson, C. W. Houchen, S. Anant, and B. K. Dieckgraefe. 2006. Dysregulation of Reg gene expression occurs early in gastrointestinal tumorigenesis and regulates anti-apoptotic genes. *Cancer Biol. Ther.* 5: 1714–1720.
31. Jung, H. C., L. Eckmann, S. K. Yang, A. Panja, J. Fierer, E. Morzycka-Wroblewska, and M. F. Kagnoff. 1995. A distinct array of proinflammatory cytokines is expressed in human colon epithelial cells in response to bacterial invasion. *J. Clin. Invest.* 95: 55–65.
32. Pickert, G., C. Neufert, M. Leppkes, Y. Zheng, N. Wittkopf, M. Warntjen, H. A. Lehr, S. Hirth, B. Weigmann, S. Wirtz, et al. 2009. STAT3 links IL-22 signaling in intestinal epithelial cells to mucosal wound healing. *J. Exp. Med.* 206: 1465–1472.
33. Wang, L., T. Yi, M. Kortylewski, D. M. Pardoll, D. Zeng, and H. Yu. 2009. IL-17 can promote tumor growth through an IL-6-Stat3 signaling pathway. *J. Exp. Med.* 206: 1457–1464.
34. Hyun, Y. S., D. S. Han, A. R. Lee, C. S. Eun, J. Youn, and H. Y. Kim. 2012. Role of IL-17A in the development of colitis-associated cancer. *Carcinogenesis* 33: 931–936.
35. Dieleman, L. A., M. J. Palmen, H. Akol, E. Bloemena, A. S. Peña, S. G. Meuwissen, and E. P. Van Rees. 1998. Chronic experimental colitis in-

duced by dextran sulphate sodium (DSS) is characterized by Th1 and Th2 cytokines. *Clin. Exp. Immunol.* 114: 385–391.
36. Fleetwood, A. J., A. D. Cook, and J. A. Hamilton. 2005. Functions of granulocyte-macrophage colony-stimulating factor. *Crit. Rev. Immunol.* 25: 405–428.
37. Hamilton, J. A. 2002. GM-CSF in inflammation and autoimmunity. *Trends Immunol.* 23: 403–408.
38. Goldstein, J. I., D. J. Kominsky, N. Jacobson, B. Bowers, K. Regalia, G. L. Austin, M. Yousefi, M. T. Falta, A. P. Fontenot, M. E. Gerich, et al. 2011. Defective leukocyte GM-CSF receptor (CD116) expression and function in inflammatory bowel disease. *Gastroenterology* 141: 208–216.
39. Uchida, K., D. C. Beck, T. Yamamoto, P. Y. Berclaz, S. Abe, M. K. Staudt, B. C. Carey, M. D. Filippi, S. E. Wert, L. A. Denson, et al. 2007. GM-CSF autoantibodies and neutrophil dysfunction in pulmonary alveolar proteinosis. *N. Engl. J. Med.* 356: 567–579.
40. Han, X., K. Uchida, I. Jurickova, D. Koch, T. Willson, C. Samson, E. Bonkowski, A. Trauernicht, M. O. Kim, G. Tomer, et al. 2009. Granulocyte-macrophage colony-stimulating factor autoantibodies in murine ileitis and progressive ileal Crohn's disease. *Gastroenterology* 136: 1261–1271, e1–3.
41. Dieckgraefe, B. K., and J. R. Korzenik. 2002. Treatment of active Crohn's disease with recombinant human granulocyte-macrophage colony-stimulating factor. *Lancet* 360: 1478–1480.
42. Korzenik, J. R., B. K. Dieckgraefe, J. F. Valentine, D. F. Hausman, and M. J. Gilbert; Sargramostim in Crohn's Disease Study Group. 2005. Sargramostim for active Crohn's disease. *N. Engl. J. Med.* 352: 2193–2201.
43. Valentine, J. F., R. N. Fedorak, B. Feagan, P. Fredlund, R. Schmitt, P. Ni, and T. J. Humphries. 2009. Steroid-sparing properties of sargramostim in patients with corticosteroid-dependent Crohn's disease: a randomised, double-blind, placebo-controlled, phase 2 study. *Gut* 58: 1354–1362.